3D Thermography Imaging Standardization Technique for Inflammation Diagnosis

Xiangyang Ju[1] Jean-Christophe Nebel[2] J. Paul Siebert[1]
Department of Computing Science, University of Glasgow, Glasgow G12 8QQ, UK[1]
Digital Imaging Research Centre, School of Computing & Information Systems, Kingston University Kingston upon Thames, Surrey, KT1 2EE, UK[2]
{xju@dcs.gla.ac.uk j.nebel@kingston.ac.uk psiebert@dcs.gla.ac.uk}

ABSTRACT

We develop a 3D thermography imaging standardization technique to allow quantitative data analysis. Medical Digital Infrared Thermal Imaging is very sensitive and reliable mean of graphically mapping and display skin surface temperature. It allows doctors to visualise in colour and quantify temperature changes in skin surface. The spectrum of colours indicates both hot and cold responses which may co-exist if the pain associate with an inflammatory focus excites an increase in sympathetic activity. However, due to thermograph provides only qualitative diagnosis information, it has not gained acceptance in the medical and veterinary communities as a necessary or effective tool in inflammation and tumor detection. Here, our technique is based on the combination of visual 3D imaging technique and thermal imaging technique, which maps the 2D thermography images on to 3D anatomical model. Then we rectify the 3D thermogram into a view independent thermogram and conform it a standard shape template. The combination of these imaging facilities allows the generation of combined 3D and thermal data from which thermal signatures can be quantified.

Keywords: Thermography, Thermogram Standardization, 3D imaging, Inflammation

1. INTRODUCTION

All objects with a temperature above absolute zero emit infrared radiation defined by the Stefan-Boltzmann Law which states that the total radiation emitted by an object is directly proportional to the object's area and emissivity and the fourth power of its absolute temperature. Medical Digital Infrared Imaging, otherwise known as clinical thermography is based on a careful analysis of skin surface temperatures as a reflection of normal or abnormal human physiology.

For nearly half a century research has been conducted on humans [6] and animals [12] showing the correlation between temperature patterns and medical conditions. The temperature of an area of the body is a product of cell metabolism and local blood flow and increases in temperature are usually the result of an increase in these factors, although blood flow plays the major role. With some disease processes there is a reduction in blood flow to the affected tissues and this will also result in alterations in surface temperature. In particular extensive research has studied skin surface temperature associated with breast cancer. In 1963, Lawson and Chughtai published a study demonstrating that the increase in regional skin surface temperature associated with breast cancer was related to both increased vascular flow and increased metabolism [7]. In 1982, thermography was approved by the U.S. Food and Drug Administration (FDA) as a supplement to mammography in helping to detect breast cancer.

Though thermography is FDA approved, this procedure, which is cheap and non-invasive no radiation or intravenous injection is used – (examinations could be performed as often as indicated), has *not* gained acceptance in the medical and veterinary communities as a necessary or effective tool in inflammation and tumour detection. Thermographic examination must be conducted in a rigorously controlled environment to prevent the introduction of artifacts. First of all, they must be able to stand up and corroborate the evidence provided by more established techniques. There has been

no objective work published on reproducibility, both within individual cases and between animals of the same species that can provide a normal base line for other users to refer to. Wakamiya [14] converted thermograms to a uniform shape to standardize the thermograms but the method could not avid the problem that the thermograms were view dependent.

We propose to combine 3D surface models with 2D thermal images to generate 3D thermograph. This firstly enables us to measure quantitatively the heat flux emitted from the surface of a subject [1] and the secondly allow us to standardize the thermograph for comparison or statistical analysis. Measuring the 3D surface enables us to compute the orientation and distance and between the camera and the surface of the subject hence allows us to quantify the actual heat flux emitted per unit surface area. Standardization is achieve through a conformation technique previous designed for human body animation [3] and shape analysis [5, 9]. Standardized thermograms can be used to create active appearance model for statistical analysis [13] and to create a normal base line.

2. DATE CAPTURE AND 3D MODEL GENERATION

2.1 Principle

A 3D thermogram scanner is a piece of technology that has the capability of capturing 3D and infrared data in a synchronized manner: it does combine a 3D scanner and a thermal camera. Its configuration is shown on Figure 1.

Figure 1: Configuration of the 3D thermogram scanner

The process of 3D capture relies upon stereo photogrammetry [10]: two high-resolution colour cameras generate colour images that are used for stereo range finding. And the infrared image is used to capture the thermal signature of the subject.

2.2 Hardware

2.2.1 Stereo pair of colour cameras

We use two high-resolution colour cameras, which are commercially available: Mamiya RZ67 PRO II, 6x7 cm SLR camera series connected to Kodak Professional DCS Pro Backs. Inside these ProBacks, there is a 16 megapixel sensor

(4080x4080) generating a 48MB file. Moreover capture software was written using the ProBack SDK in order to synchronize the capture of the stereo pair of cameras.

Figure 2: Colour camera used in the stereo pair

2.2.2 Thermal camera

Our thermal imager is an Indigo Systems Merlin Mid Camera. It uses cooled Indium Antimonide to detect infrared radiation in the 3~5 μm waveband. The camera uses a GaAs based lens in order to capture the infrared radiation, as it will not penetrate through glass. The sensitivity of 25mK associated with the detector is necessary for detailed medical observation and quantification of heat flux. Moreover the response time of such detectors is in milliseconds, which allows the capture of real-time thermal signatures.

Figure 3: Thermal camera

2.3 3D Data generation

In order to build 3D models from the data captured by the scanner previously described, the cameras have to be calibrated, e.g. the detailed geometric configuration of all the cameras has to be known. Figure 4 shows a heated calibration target seen by the colour cameras and by the infrared camera. Then once the capture has been done, the

stereo matching process is applied to the stereo-pair images. The algorithm we use is based on multi-resolution image correlation [15].

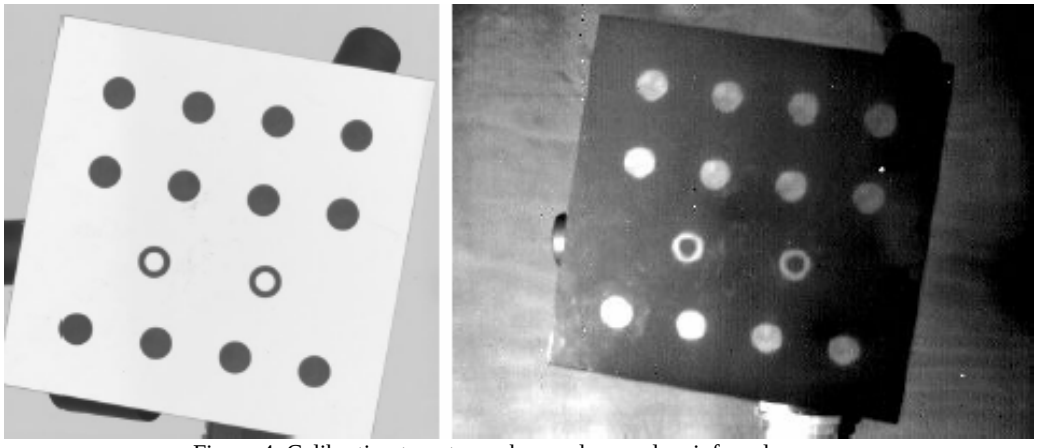

Figure 4: Calibration target seen by a colour and an infrared camera

Once the stereo matching process is completed, the final displacement files combined with the calibration file of the associated pod allow the generation of a range map, i.e. the map of the distances between each pixel and the coordinate system of the pod. An implicit surface is computed that merges together the point clouds into a single triangulated polygon mesh using a variant of the marching cubes algorithm [8]. This mesh is then further decimated to any arbitrary lower resolution for display purposes.

The generation of a 3D thermogram is achieved by mapping the infrared picture taken by the infrared camera to the 3D geometry. Since the thermal camera and the stereo pair of cameras are calibrated together the mapping phase is quite straightforward. On Figure 5(a), stereo images of left and right cameras and their corresponding thermal image are shown. The range image is constructed from the stereo pair and mapped with the thermal image (Figure 5(b)). A more detailed presentation of the 3D capture system based on high-resolution colour cameras is given by Ju [4].

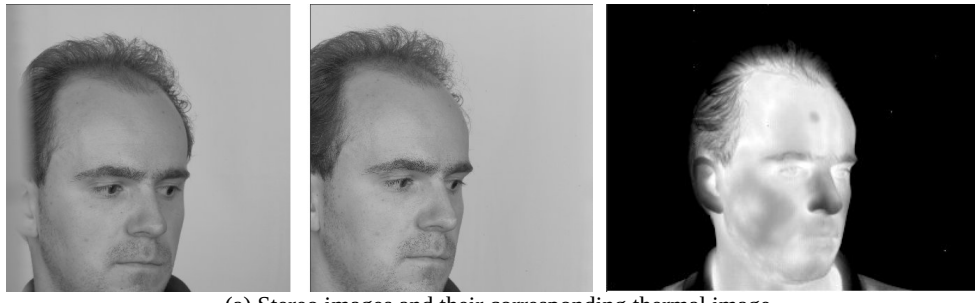

(a) Stereo images and their corresponding thermal image

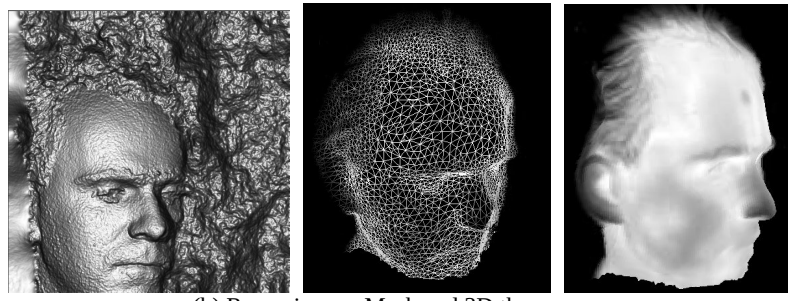

(b) Range image, Mesh and 3D thermogram

Figure 5: Views of a 3D thermogram

3. THERMOGRAM STANDARDIZATION

Thermogram standardization consists of two major steps. In the first step, the thermograms are rectified that they are view independent. In the second step, the thermograms are conformed to a standard face template to be standardized.

3.1 Thermogram rectifications

Since the heat flow measured by an infrared camera depends on the distance and the angle between the camera and the object of interest, observations depend on the position of the observer. Using the information of these 3D thermograms, we are able to rectify thermograms that they are independent from camera position.

The flux, F in watt, is the instantaneous measure of the quantity of radiation. It describes the output of a source propagating in the form of a beam or received by a detector [2]. If the radiance, L, is uniform, the flux is defined by

$$F = LSR(\cos\Phi_1 \cos\Phi_2)/d^2 \quad (1)$$

Where Φ_1 Φ_2 are the angles between the line joining the source area S, to the receptor area R, and the source surface normal N_S and the receptor surface normal N_R, respectively (see Figure 6). And d is the distance between S and R.

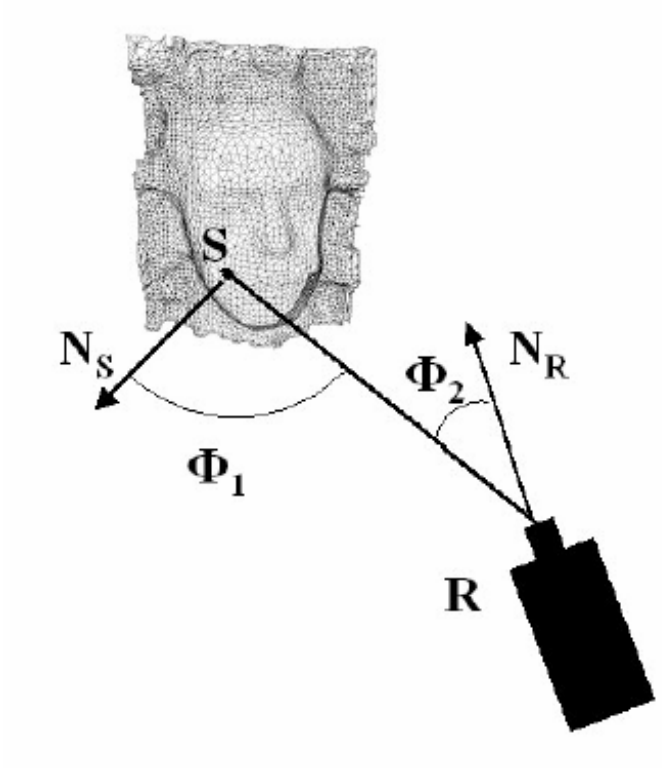

Figure 6: Flux measured by the thermal camera

The flux measured by the thermal camera depends on the angle and distance between the object and the camera. In order to generate thermograms that are view independent, we offer to create a rectified flux F_S , [1]

$$F_S = LSR = F \cdot d^2/(\cos\Phi_1 \cos\Phi_2) \quad (2)$$

3.2 Thermogram conformation

After the rectification, the thermograms are conformed to a standard facial shape template. Once thermograms are standardized, any image processing technique can be used for their analysis. A normal thermogram can be calculated from samples collected from health people. We have started to investigate the automatic detection, monitoring and quantification of inflammations. The idea is either to compare longitudinally thermographs of the same area in order to monitor the healing of an inflammation or to detect and quantify an inflammation by comparing the thermogram of interest with a normal thermogram.

The conformation consists of a landmark controlled global mapping based on radial basis functions (RBF) and a local elastic optimization. Given N landmarks on the 3D thermogram mesh $\boldsymbol{A}=\{\mathbf{a}_1, \ldots, \mathbf{a}_N\} \subset \mathbf{R}^3$ and corresponding landmarks on the facial template $\boldsymbol{S(A)} = \{\mathbf{s}_1, \ldots, \mathbf{s}_N\} \subset \mathbf{R}^3$, each vertex $\mathbf{x}$ of the generic mesh is mapped by $\boldsymbol{g(x)}$ based on RBF

$$\mathbf{g(x)} = \mathbf{p(x)} + \sum_{i=1}^{N} \lambda_i \varphi(|\mathbf{x} - \mathbf{a}_i|), \mathbf{x} \in \mathbf{R}^3, \; i = 1,2,\ldots,N \tag{3}$$

where $\mathbf{p}$ is an affine transformation, λ_i is a real-valued weight, φ is a basis function, φ, $\boldsymbol{R}^+ \rightarrow \boldsymbol{R}$, and $|\mathbf{x} - \mathbf{a}_i|$ is simply a distance. Here we select the biharmonic function $\varphi(r) = r$ as the basis function, where $r = |\mathbf{x} - \mathbf{a}_i|$.

Following global mapping, the thermogram mesh is further deformed towards the facial template locally. The deformation of the thermogram model is constrained by minimizing the global energy of the mesh,

$$E = E_{ext} + \varepsilon E_{\text{int}} \tag{4}$$

where the parameter ε controls the trade-off between geometry similarity attractions between the thermogram mesh and the facial template and physical constraints within the thermogram mesh. Full details can be found in [5, 9]. The difference between this paper and our previous conformation papers is that we focused on establishing shape correspondences before; now we focus on standardizing the thermogram. We conformed scanned 3D shape to the template. The 2D thermal image mapped on a scanned 3D face is mapped onto the standard facial template after the thermogram conformation.

4. RESULTS

After the 3D surface was reconstructed from the stereo images, the distance of the face to the thermal camera was known and the angles Φ_1 Φ_2 were calculated. Figure 7 shows a thermogram and its corresponding distance and angle maps generated using the 3D information provided by the 3D model.

Figure 7: Thermogram, distance and angle maps

Made use of the equation (2), the original thermogram was rectified. Figure 8 shows a raw thermogram and the rectified thermogram based on the assumption that pixel values are proportional to flux values. It can be noticed that areas with normal pointing away from the camera (white areas on the angle map) are much brighter on the rectified thermogram than on the original thermogram. The rectified thermogram was view independent.

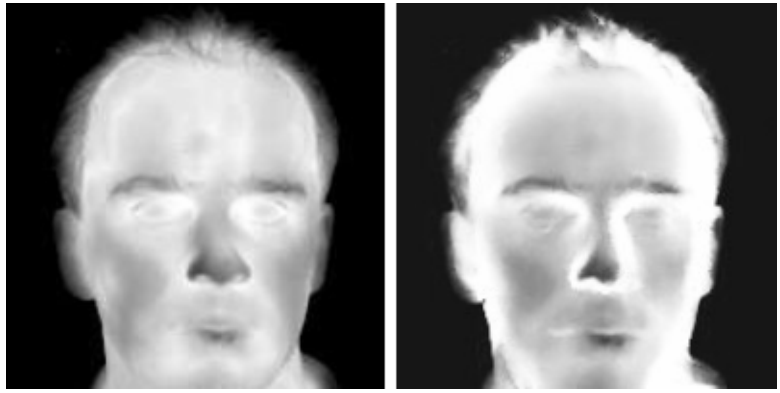

Figure 8: Original and rectified thermogram

The 3D thermogram conformed to a standard facial template is illustrated in Figure 9. Where the captured thermogram (left) conformed to the template (middle) to obtain a standardized thermogram which can compare with its own historical records or compare with other individuals. Other advantage of the standardization is that we can create a normal base line of facial thermogram from the thermograms collected from a healthy population. Active appearance model [13] can be build up.

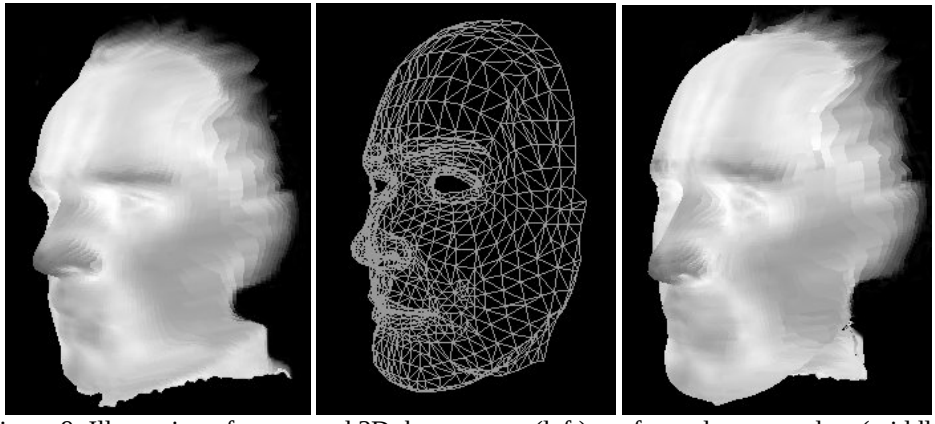

Figure 9: Illustration of a captured 3D thermogram (left) conformed to a template (middle) that results in a standardized thermogram (right)

5. CONCLUSION

We presented in this paper a 3D thermograph imaging standardization technique that combined 3D photogrammetry with 2D thermal technique. We illustrated our standardization procedure for standardizing thermograms. The standardization is obviously not limited to the facial models. Our standardization created a view independent thermogram and conformed the thermogram to a standard template for quantitative analysis. The standardization enables us to compare thermograms between the same individual and that of different persons. Also it enables us to create a normal base line of thermogram.

REFERENCES

1. P. Aksenov, I. Clark, D. Grant, A. Inman, L. Vartikovski and J.-C. Nebel. “3D Thermography for the quantification of heat generation resulting from inflammation”. Proc. 8th 3D Modelling symposium, Paris, France, 2003
2. G. Gaussorgues, Infrared Thermography, *Microwave Technology Series* 5, Chapman and Hall, London, 1994.
3. X. Ju and J. P. Siebert, “Conforming Generic Animatable Models to 3D Scanned Data”. International Conference of Numberisation 3D - Scanning 2001, 4-5 April 2001, Paris, France.[
4. X. Ju, J. P. Siebert, “High resolution stereo system”, Proc. 3D Modelling 2003, Paris, France, 2003
5. X. Ju, Z. Mao, J. P. Siebert, N. McFarlane, J. Wu, R. Tillett. “Applying Mesh Conformation on Shape Analysis with Missing Data”. 2nd International Symposium on 3D Data Processing, Visualization, and Transmission, 3DPVT 2004, IEEE Computer Society Press.
6. R. Lawson, “Implications of Surface Temperatures in the Diagnosis of Breast Cancer”. Can Med Assoc J **75**: 309-310,1956.
7. R. Lawson and M. S. Chughtai, “Breast cancer and body temperatures”. Can Med Assoc J 88: 68-70,1963.
8. W. E. Lorensen and H.e Cline, “Marching cubes: a high resolution 3D surface construction algorithm”, ACM Computer Graphics, **21**, 1987
9. Z. Mao, J. P. Siebert, W. P. Cockshott, A. F. Ayoub. “Constructing Dense Correspondences to Analyze 3D Facial Change”. 17th International Conference on Pattern Recognition, ICPR2004, Vol **3**. IEEE Computer Society Press.
10. J. P. Siebert and S. J. Marshall, “Human body 3D imaging by speckle texture projection photogrammetry”, Sensor Review **20** (3), p.p. 218-226, 2000.
11. S. T. Smith, Modelling Hot Bodies: “Combined real-time 3D and Thermal Imaging for Medical Applications”, Information Technology, MSc IT project report, Glasgow Univ., 2002.
12. B. Stromberg, “The use of thermography in equine orthopedics”. J Vet Radiol 1974.
13. T. F. Cootes, Gareth J. Edwards, C. J. Taylor. “Active Appearance Models”. IEEE Transactions On Pattern Analysis And Machine Intelligence, 23(6), JUNE 2001. pp681-685.
14. J. Wakamiya. “Data Processing Method for Standardizationof Thermographic Diagnosis”. IEEE Engineering in Medicine & Biology. The 22nd Annual International Conference. Navy Pier Convention Center, Chicago, Il USA, July23-28, 2000.
15. J. Zhengping, “On the multi-scale iconic representation for low-level computer vision systems”. PhD thesis, The Turing Institute and The University of Strathclyde, 1988.